

## ORIGINAL ARTICLE

# SHOC2 subcellular shuttling requires the KEKE motif-rich region and N-terminal leucine-rich repeat domain and impacts on ERK signalling

Marialetizia Motta<sup>1</sup>, Giovanni Chillemi<sup>2</sup>, Valentina Fodale<sup>3,†</sup>,  
Serena Cecchetti<sup>4</sup>, Simona Coppola<sup>5</sup>, Silvia Stipo<sup>3</sup>, Viviana Cordeddu<sup>3</sup>,  
Pompeo Macioce<sup>4</sup>, Bruce D. Gelb<sup>6</sup> and Marco Tartaglia<sup>1,\*</sup>

<sup>1</sup>Genetics and Rare Diseases Research Division, Ospedale Pediatrico Bambino Gesù, Rome, Italy, <sup>2</sup>CINECA, SCAI-SuperComputing Applications and Innovation Department, Rome, Italy, <sup>3</sup>Department of Hematology, Oncology and Molecular Medicine, <sup>4</sup>Department of Cell Biology and Neurosciences, <sup>5</sup>Italian National Centre for Rare Diseases, Istituto Superiore di Sanità, Rome, Italy and <sup>6</sup>The Mindich Child Health and Development Institute, Icahn School of Medicine at Mount Sinai, New York, NY, USA

\*To whom correspondence should be addressed at: Marco Tartaglia, Genetics and Rare Diseases Research Division, Ospedale Pediatrico Bambino Gesù - IRCCS, Viale di San Paolo, 15 00146 Rome, Italy. Tel: +39-06-6859-3742; Email: marco.tartaglia@opbg.net

## Abstract

SHOC2 is a scaffold protein composed almost entirely by leucine-rich repeats (LRRs) and having an N-terminal region enriched in alternating lysine and glutamate/aspartate residues (KEKE motifs). SHOC2 acts as a positive modulator of the RAS-RAF-MEK-ERK signalling cascade by favouring stable RAF1 interaction with RAS. We previously reported that the p.Ser2Gly substitution in SHOC2 underlies Mazzanti syndrome, a RASopathy clinically overlapping Noonan syndrome, promoting N-myristoylation and constitutive targeting of the mutant to the plasma membrane. We also documented transient nuclear translocation of wild-type SHOC2 upon EGF stimulation, suggesting a more complex function in signal transduction. Here, we characterized the domains controlling SHOC2 shuttling between the nucleus and cytoplasm, and those contributing to SHOC2<sup>S2G</sup> mistargeting to the plasma membrane, analysed the structural organization of SHOC2's LRR motifs, and determined the impact of SHOC2 mislocalization on ERK signalling. We show that LRRs 1 to 13 constitute a structurally recognizable domain required for SHOC2 import into the nucleus and constitutive targeting of SHOC2<sup>S2G</sup> to the plasma membrane, while the KEKE motif-rich region is necessary to achieve efficient SHOC2 export from the nucleus. We also document that SHOC2<sup>S2G</sup> localizes both in raft and non-raft domains, and that it translocates to the non-raft domains following stimulation. Finally, we demonstrate that SHOC2 trapping at different subcellular sites has a diverse impact on ERK signalling strength and dynamics, suggesting a dual counteracting modulatory role of SHOC2 in the control of ERK signalling exerted at different intracellular compartments.

<sup>†</sup>Present address: IRBM Promidis, Pomezia, Rome, Italy.

Received: May 16, 2016. Revised: July 4, 2016. Accepted: July 8, 2016

© The Author 2016. Published by Oxford University Press.

All rights reserved. For Permissions, please email: journals.permissions@oup.com

## Introduction

SHOC2 (also known as SUR-8 and SOC-2) is a widely expressed protein composed almost entirely of leucine-rich repeats (LRRs), and having a region rich in alternating lysine and glutamate (or aspartate) residues (KEKE motifs) at the N-terminus. In *C. elegans*, where it was originally discovered, the protein acts as a positive modulator of intracellular signalling elicited by cell-surface receptor kinases and mediated by LET-60, the homolog of vertebrate RAS sub-family GTPases (1,2). Since LRRs provide a structural framework for protein-protein interactions (3), SHOC2 is believed to function as a scaffold protein linking RAS proteins to downstream signal transducers (4,5). This view has been confirmed by the observation that SHOC2 functions as a regulatory protein of the catalytic subunit of protein phosphatase 1 (PP1C) (6). By binding GTP-bound MRAS, SHOC2 promotes PP1C translocation to the membrane, allowing PP1C-mediated dephosphorylation of RAF1 at a major inhibitory residue, Ser<sup>259</sup>, which is a required event for stable RAF1 binding to activated GTP-bound RAS, RAF1 catalytic activation and efficient transmission of signalling through MEK and ERK proteins (6).

The relevance of SHOC2's function on RAS-RAF-MEK-ERK (RAS-MAPK, hereafter) signalling has been further highlighted by the discovery that a single missense mutation (c.4A > G, p.Ser2Gly) in SHOC2 underlies Mazzanti syndrome (MIM 607721; also known as Noonan syndrome-like disorder with loose anagen hair) (7), a disorder affecting development and growth clinically overlapping Noonan syndrome (MIM 163950), the most common RASopathy (8,9). Similar to other RASopathies, Mazzanti syndrome is characterized by reduced postnatal growth, variable cognitive deficits, congenital cardiac defects, and ectodermal anomalies (7,10). Biochemical and functional studies demonstrated that the disease-causing mutation creates an N-myristoyltransferase (NMT) recognition site driving aberrant N-myristoylation of SHOC2<sup>S2G</sup>, its constitutive plasma membrane targeting, and enhanced ERK activation in a cell type-specific fashion (7).

N-terminal myristoylation is an irreversible form of protein fatty acylation occurring co-translationally in which myristate, a 14-carbon saturated fatty acid, is covalently added to an N-terminal glycine residue of a nascent polypeptide after excision of the initiator methionine residue by methionyl aminopeptidase (11,12). N-myristoylation is a relatively common lipid modification of many membrane-bound signal transducers (13,14). While it contributes to protein anchoring to cellular membranes, the binding energy it provides is relatively weak and not sufficient *per se* to promote stable binding of proteins to the membrane (15). In N-myristoylated membrane-anchored proteins, a second signal, either a polybasic residue stretch or a palmitoylation recognition motif, is commonly observed (14,16). The former contributes to stabilize protein binding to the membrane via electrostatic interactions with the head groups of acidic phospholipids of the cytoplasmic leaflet of the bilayer (17,18), while the latter favours a strong association with the lipid bilayer by increasing protein hydrophobicity (19,20). Alternatively, membrane interaction of singly acylated proteins can be enhanced by interactions with other membrane bound proteins. Similarly, N-myristoylation does not contain the information required to direct targeting specifically to the cytoplasmic side of the plasma membrane (or to other intracellular membranes), which requires additional events that are usually mediated by membrane-bound proteins and enzymes (13,14).

While growth factor-induced translocation of SHOC2 to the membrane is largely accepted as a required event promoting efficient RAS-mediated ERK activation, we noticed that SHOC2 is

uniformly distributed in the cytoplasm and nucleus in resting conditions, and that it translocates to the nucleus following EGF stimulation (7). These observations suggest that SHOC2 may have multiple regulatory roles in intracellular signalling. The structural elements mediating SHOC2 nucleo-cytoplasm shuttling and the impact of its different subcellular localization on RAS-MAPK signalling have not been characterized yet.

In this study, we explored the mechanisms mediating plasma membrane targeting of the RASopathy-causing SHOC2<sup>S2G</sup> mutant and EGF-dependent nuclear-cytoplasm shuttling of wild-type SHOC2, as well as the impact of SHOC2 intracellular mislocalization on ERK signalling. We show that the N-terminal LRRs mediate SHOC2 import into the nucleus and constitutive targeting of myristoylated SHOC2<sup>S2G</sup> to the plasma membrane, while the C-terminal LRRs do not significantly impact on subcellular compartmentalization. Consistently, we provide evidence that SHOC2's LRRs are organized into two structurally independent domains that are connected by a flexible hinge constituted by the variable region of LRR 13. We also show that the N-terminal KEKE motif-rich region is required for efficient SHOC2 export from the nucleus. Finally, we demonstrate that while nuclear trapping of SHOC2 is associated with less efficient activation of ERK, its impaired nuclear import results in prolonged activation of the kinase, suggesting a previously unrecognized negative modulatory role of SHOC2 in the control of ERK signalling exerted in the nucleus.

## Results

### SHOC2 nuclear import is not mediated by conventional nuclear localization sequences

While nucleocytoplasmic trafficking of small proteins is generally achieved by passive diffusion through the nuclear pore complex, larger proteins or protein complexes necessitate active transport (21). Nuclear import generally requires the recognition of a nuclear localization signal (NLS) by the transport machinery, and multiple 'monopartite' and 'bipartite' NLSs have been identified. The PSORTII (<http://psort.hgc.jp/>) and Wregex (<http://wregex.ehubio.es/faces/home.xhtml>) WEB servers were used to scan the SHOC2 sequence to recognize potential NLS motifs. While no putative bipartite NLS was detected, a single monopartite NLS (PGTRKKS at position 79), satisfying the consensus sequence of the Pat7 motif (i.e. PX<sub>1-3</sub>-K/R<sub>3-4</sub>) was identified. To validate this putative NLS functionally, a SHOC2 mutant (SHOC2<sup>P79A/R82G/K83G</sup>) carrying multiple substitutions affecting key residues of the motif was generated (Figure 1), and subcellular localization in starved and EGF-stimulated transfected COS-1 cells was analysed by confocal laser scanning microscopy. Similar to what was observed for the wild-type protein, SHOC2<sup>P79A/R82G/K83G</sup> efficiently translocated to the nucleus following growth factor stimulation and was uniformly distributed in the cytoplasm and nucleus during starvation (Figure 2A, panels a and b). This subcellular distribution pattern was confirmed by cell fractionation experiments (Figure 2B), excluding the role of this motif in mediating nuclear import of the protein and indicating that SHOC2 does not contain a functionally active conventional NLS mediating nuclear import.

### Role of KEKE motifs and LRRs in SHOC2's subcellular localization

SHOC2 is characterized by two distinct regions that are believed to mediate binding of the protein to signalling partners (Figure

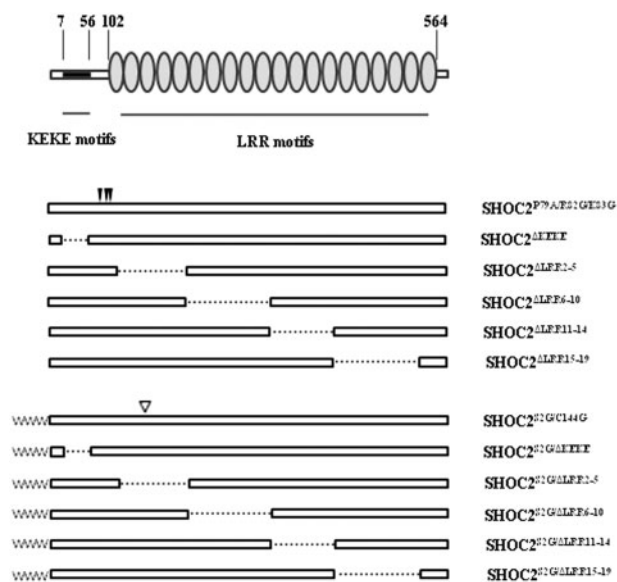


**Figure 1.** SHOC2 protein structure and list of the generated mutants. SHOC2 is characterized by an N-terminal region enriched in alternating lysine and glutamate/aspartate residues (KEKE motifs) (black) followed by 20 repeats (LRRs) (gray). Numbers above the domain structure indicate the amino acid boundaries of those domains. The generated mutants for the wild-type protein (middle panel) and the RASopathy-causing mutant (bottom panel) are shown. P79A/R82G/K83G, nuclear localization sequence mutant; ΔKEKE, KEKE motifs-rich region deleted mutant; ΔLRR2-5, ΔLRR6-10, ΔLRR11-14 and ΔLRR15-19, LRRs deleted mutants; C144G, putative palmitoylation site mutant.

1). At the N-terminus, a low-complexity and highly charged stretch (residues 7 to 56) contains multiple KEKE motifs that have been proposed to represent association domains or polar zippers involved in protein-protein association (22,23). The second region, which embraces most of the SHOC2's sequence (residues 102-564), counts 20 tandemly arranged LRR motifs (Supplementary Material, Table S1), which are known to constitute a versatile module involved in protein-protein interactions. To identify the domains implicated in SHOC2's nucleocytoplasmic shuttling, several mutants lacking the N-terminal region encompassing the KEKE motifs (SHOC2<sup>ΔKEKE</sup>) or different subsets of LRRs (SHOC2<sup>ΔLRR2-5</sup>, SHOC2<sup>ΔLRR6-10</sup>, SHOC2<sup>ΔLRR11-14</sup> and SHOC2<sup>ΔLRR15-19</sup>) were generated (Figure 1). The subcellular localization of each mutant was examined by confocal microscopy in transiently transfected COS-1 cells during starvation or following growth factor stimulation, and validated by cell fractionation experiments. Western blot analysis confirmed that all mutants were efficiently expressed, although a relatively reduced level was observed for the SHOC2<sup>ΔLRR2-5</sup> and SHOC2<sup>ΔLRR15-19</sup> proteins (Supplementary Material, Fig. S1). Significantly, diverse distribution patterns were observed for the different mutants. Specifically, SHOC2<sup>ΔKEKE</sup> showed constitutive nuclear localization, indicating retention of the mutant in the nucleus and providing evidence for a role of the N-terminal KEKE motif-rich region in the process mediating nuclear export of SHOC2 to the cytoplasm (Figure 2A, panel c). A perturbed subcellular localization was also observed for two of the four mutants with partial deletions of the LRR region, SHOC2<sup>ΔLRR2-5</sup> and SHOC2<sup>ΔLRR6-10</sup>. Those mutants showed a distribution restricted to the cytoplasm during starvation and impaired nuclear translocation following EGF stimulation (Figure 2A, panels d and e). In contrast to the constitutive retention in the cytoplasm of those mutants, SHOC2<sup>ΔLRR11-14</sup> and SHOC2<sup>ΔLRR15-19</sup>, which lack

more C-terminally positioned LRRs, displayed an intracellular distribution that grossly overlapped that of wild-type protein in both serum starved and EGF stimulated cells (Figure 2A, panels f and g). These observations were confirmed using different cell lines (Neuro2A and HEK293) (data not shown). The impaired export from the nucleus of the SHOC2<sup>ΔKEKE</sup> mutant and the cytoplasmic localization of the SHOC2<sup>ΔLRR2-5</sup> protein were confirmed by cell fractionation assays (Figure 2B).

Overall, these findings indicate that the first 10 LRRs are required for the transport of SHOC2 from the cytoplasm to the nucleus, while the N-terminal KEKE motif-rich region mediates nuclear export of the protein.

### SHOC2 mutants lacking the KEKE motif-rich region and those missing the N-terminal LRRs impact RAS-MAPK signalling differently

Multiple lines of evidence support the view that SHOC2's positive modulatory role on RAS-MAPK signalling is linked to its translocation to the plasma membrane and promotion of RAF1 stable interaction with GTP-bound RAS proteins. To explore the impact of forced nuclear localization and constitutive retention in the cytoplasm of SHOC2 on ERK activation, we analysed the levels of ERK phosphorylation associated with the overexpression of the SHOC2 mutants lacking different LRR motifs in Neuro2A cells, a line for which the capability of SHOC2 to modulate ERK signalling had previously been demonstrated (7). Following EGF stimulation, overexpression of wild-type SHOC2 resulted in greater ERK phosphorylation compared with what was observed in untransfected cells. As expected, nuclear trapping of the protein resulted in a less efficient activation of ERK (Figure 2C), which is consistent with the required SHOC2-mediated translocation of PP1C to the plasma membrane (or other intracellular membranes) for efficient RAF1 binding to activated RAS, and RAF1 activation. In contrast, impaired nuclear import of SHOC2 was associated with a more sustained activation of ERK (Figure 2C and Supplementary Material, Fig. S2), suggesting a possible involvement of the protein in MAPK signal switch-off, in the nucleus. The specific role of the N-terminal LRRs in this unpredicted effect on ERK phosphorylation was confirmed by the observation that overexpression of SHOC2<sup>ΔLRR11-14</sup> and SHOC2<sup>ΔLRR15-19</sup> resulted in an ERK phosphorylation pattern that was similar in amplitude and duration to that observed in cells transfected with the wild-type protein (Figure 2C and Supplementary Material, Fig. S2). These findings were confirmed by ELK1-driven transactivation assay experiments performed in NIH 3T3 cells used as a readout of MAPK activation (Supplementary Material, Fig. S3).

These data indicate that the specific intracellular localization of SHOC2 differentially impacts RAS-MAPK signalling and that besides the positive role on MAPK signalling associated with the activation of RAF1, SHOC2 might contribute to the switch-off of MAPK signalling, following its translocation to the nucleus.

### Dual acylation is not implicated in stable plasma membrane binding of SHOC2<sup>S2G</sup>

According to the 'two-signal model' for membrane binding of N-myristoylated proteins, stable membrane association and targeting specificity are generally achieved by either a polybasic residue stretch or a second acylation event (i.e. palmitoylation) (13). Interaction with other membrane-bound proteins might

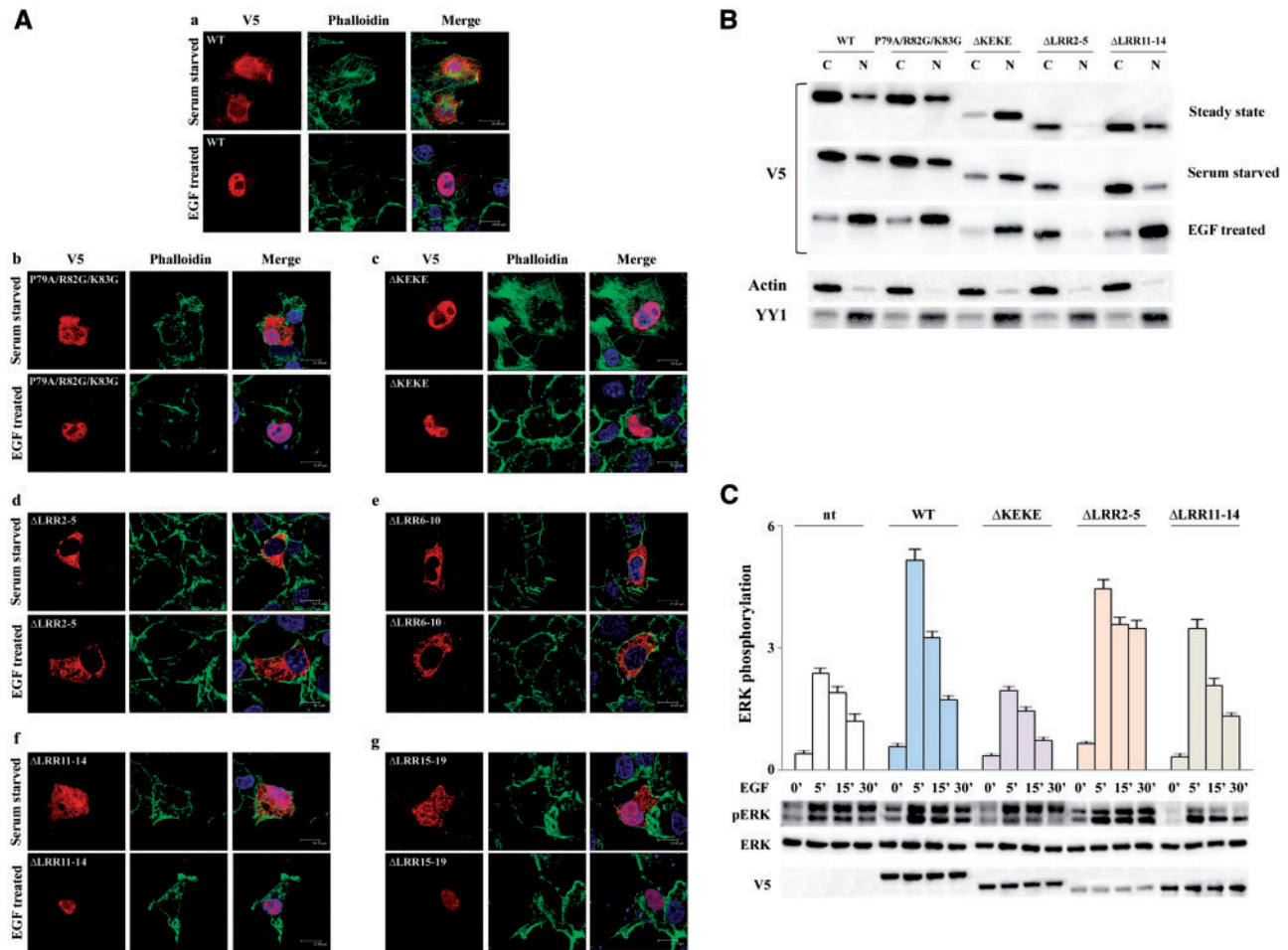


**Figure 2.** Subcellular localization of the generated SHOC2 mutants, and their effect on ERK signalling. (A) Localization of the transiently expressed mutants in COS-1 cells during starvation or following growth factor stimulation revealed by confocal microscopy. (B) Localization of the transiently expressed mutants in COS-1 cells cultured in steady state, serum starved and EGF treated conditions, determined by cell fractionation experiments (C, cytoplasm; N, nucleus). (C) Western blot analysis documenting the levels of ERK phosphorylation associated with the overexpression of wild-type SHOC2 or a selected subset of mutants in Neuro2A cells in time-course EGF stimulation experiments.

also stabilize targeting to specific membrane domains. The N- and C-terminal region of SHOC2 contain neither a net positively charged region potentially implicated in phospholipids binding nor cysteine residues, excluding the role of palmitoylation, farnesylation, geranylgeranylation and other lipid anchors as post-translational modifications contributing to stable interaction with the lipid bilayer in the mutant. Similarly, the CSS-Palm v4.0 prediction tool (<http://csspalm.biocuckoo.org/>) did not identify any consensus motif predicted with high confidence for reversible S-palmitoylation throughout the SHOC2 sequence. A few putative palmitoylation sites (Cys<sup>144</sup>, Cys<sup>238</sup>, Cys<sup>342</sup> and Cys<sup>540</sup>) were called with low confidence. To exclude this possibility experimentally, the best candidate site among those was assayed by evaluating the subcellular localization of the SHOC2<sup>S2G/C144G</sup> double mutant by confocal microscopy in transiently transfected COS-1 cells. Similarly to SHOC2<sup>S2G</sup>, the protein was efficiently expressed and exhibited a constitutive plasma membrane localization, indicating that palmitoylation at Cys<sup>144</sup> does not occur or does not contribute to stable membrane binding of myristoylated SHOC2<sup>S2G</sup> (Figure 3A, panels a and b). A membrane-restricted distribution of the SHOC2<sup>S2G/C144G</sup> mutant was consistently observed also in cell fractionation assays (Figure 3B).

These analyses strongly suggested that SHOC2<sup>S2G</sup> targeting to the plasma membrane likely depends on specific interactions with membrane-bound proteins.

### Role of KEKE motifs and LRRs in SHOC2<sup>S2G</sup> subcellular localization

To assess the possible contribution of the LRR motifs in driving plasma membrane targeting of SHOC2<sup>S2G</sup>, four mutants carrying partial deletions of the LRR domain were generated (Figure 1), and their subcellular localization was examined in transfected COS-1 cells during starvation and following EGF stimulation. Among these mutants, SHOC2<sup>S2G/ΔLRR2-5</sup> and SHOC2<sup>S2G/ΔLRR15-19</sup> were poorly expressed, which was due, in part, to their reduced stability and accelerated degradation via the proteasome (Supplementary Material, Fig. S1). SHOC2<sup>S2G/ΔLRR2-5</sup> and SHOC2<sup>S2G/ΔLRR6-10</sup> proteins displayed constitutive cytoplasmic localization (Figure 3A, panels d and e), establishing the requirement of these LRRs in SHOC2<sup>S2G</sup> targeting to the plasma membrane. Of note, this distribution pattern overlapped with that observed for the SHOC2<sup>ΔLRR2-5</sup> and SHOC2<sup>ΔLRR6-10</sup> mutants, pointing out an equivalent protein-protein interaction-mediated mechanism involving these motifs in the control of both

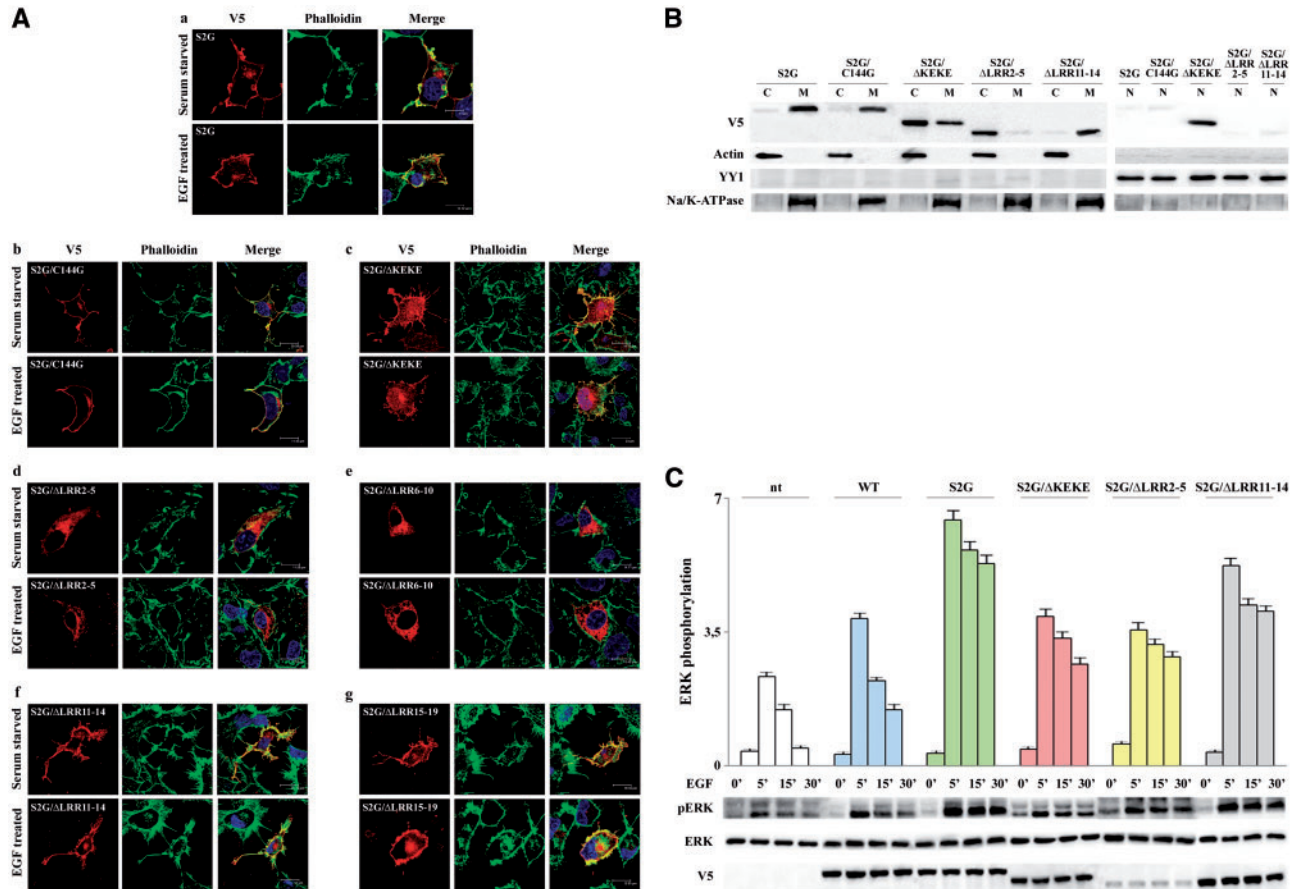


**Figure 3.** Subcellular localization of the generated SHOC2<sup>S2G</sup> mutants, and their effect on ERK signalling. (A) Localization of the transiently expressed mutants in COS-1 cells during starvation or following growth factor stimulation revealed by confocal microscopy. (B) Localization of the transiently expressed mutants in COS-1 cells under basal conditions determined by cell fractionation experiments (C, cytoplasm; M, plasma membrane; N, nucleus). (C) Western blot analysis documenting the levels of ERK phosphorylation associated with the overexpression of the RASopathy-causing mutant SHOC2<sup>S2G</sup> or a selected subset of its mutants expressed in Neuro2A cells in time-course EGF stimulation experiments.

SHOC2 translocation to the plasma membrane and its import to the nucleus. Consistent with the minor impact of the deletions of LRRs 11–14 and LRRs 15–19 in altering SHOC2 subcellular localization, SHOC2<sup>S2G/ΔLRR11-14</sup> and SHOC2<sup>S2G/ΔLRR15-19</sup> proteins localized constitutively to the plasma membrane (Figure 3A, panels f and g), demonstrating that the C-terminal LRRs are not essential for the constitutive targeting to the membrane of SHOC2<sup>S2G</sup>, and more generally do not play a major role in controlling SHOC2 intracellular trafficking. The impact of deletions on SHOC2<sup>S2G</sup> translocation to the plasma membrane was confirmed by cell fractionation assays (Figure 3B).

In sharp contrast with the other SHOC2<sup>S2G</sup> mutants, deletion of the N-terminal KEKE motifs-rich region unexpectedly resulted in the distribution of the mutant protein more widely throughout the cell (i.e. plasma membrane, cytoplasm and nucleus) (Figure 3A, panel c). The spread and spotted distribution in the cytoplasm of the SHOC2<sup>S2G/ΔKEKE</sup> mutant was suggestive of a non-specific interaction with intracellular membranes, indicating a specific contribution of this region in stabilizing SHOC2<sup>S2G</sup> targeting to the plasma membrane; on the other hand, its nuclear localization suggested the possibility of defective N-myristoylation of the mutant. To verify this hypothesis, SHOC2<sup>S2G/ΔKEKE</sup>'s myristoylation status was evaluated and compared with that of the SHOC2<sup>S2G</sup> and SHOC2<sup>S2G/ΔLRR2-5</sup> proteins. Differently from SHOC2<sup>S2G</sup> and the SHOC2<sup>S2G/ΔLRR2-5</sup> mutant,

which showed efficient [<sup>3</sup>H]myristic acid incorporation, N-myristoylation of the SHOC2<sup>S2G/ΔKEKE</sup> mutant was reduced (Supplementary Material, Fig. S4), indicating a less efficient recognition by NMT and the requirement of a more 'extended' sequence compared to what generally observed in naturally occurring N-myristoylated proteins.

### Impaired plasma membrane binding of SHOC2<sup>S2G</sup> abolishes the gain-of-function effect of SHOC2's N-myristoylation on MAPK signalling

We originally hypothesized that the RASopathy-causing Ser-to-Gly change at codon 2 in SHOC2 promotes enhanced signalling through the MAPK cascade, driving constitutive targeting of the mutant to the plasma membrane. To further validate this hypothesis, the dynamics of ERK phosphorylation were analysed in time-course experiments in EGF-stimulated Neuro2A cells transiently transfected to express SHOC2<sup>S2G</sup> mutants carrying different deletions of the LRR region or lacking the KEKE motif-rich sequence (Figure 3C and Supplementary Material, Fig. S2). In agreement with our previously reported data (7), SHOC2<sup>S2G</sup> expression was found to promote boosted and sustained EGF-dependent ERK phosphorylation compared to what was observed in cells expressing the wild-type protein.

Phosphorylation of ERK in cells expressing the SHOC2<sup>S2G/ALRR2-5</sup> and SHOC2<sup>S2G/ALRR6-10</sup> mutants was similar in amplitude to what observed in cells transfected with wild-type SHOC2 (Figure 3C and Supplementary Material, Fig. S2), providing further evidence for the requirement of plasma membrane targeting of SHOC2<sup>S2G</sup> for its role in enhancing MAPK signalling following EGF stimulation. On the other hand, sustained ERK phosphorylation was apparent in cells expressing the SHOC2<sup>S2G/ALRR2-5</sup> and SHOC2<sup>S2G/ALRR6-10</sup> mutants following stimulation (Figure 3C and Supplementary Material, Fig. S2). This dynamic, which is consistent with the effect of these mutants in promoting prolonged stimulus-dependent ERK phosphorylation, further emphasizes the relevance of nuclear translocation of SHOC2 in switching off MAPK signalling. The levels and dynamics of ERK activation in cells expressing SHOC2<sup>S2G/ALRR11-14</sup> and SHOC2<sup>S2G/ALRR15-19</sup> were comparable to those were observed in SHOC2<sup>S2G</sup> transfected cells, supporting a minor impact of the C-terminal portion of the LRR region in mediating the events controlling SHOC2's function in RAS-MAPK signalling (Figure 3C and Supplementary Material, Fig. S2), which is in line with its apparently negligible influence on SHOC2 subcellular localization. The milder impact on MAPK signalling of the deletions involving LRRs 11-14 and LRRs 15-19 compared to those affecting LRRs 2-5 and LRRs 6-10 was also confirmed by ELK1 transactivation assay experiments (Supplementary Material, Fig. S3). Finally, a less efficient but sustained ERK activation was observed for the SHOC2<sup>S2G/ΔKEKE</sup>, which would be consistent with the less efficient plasma membrane targeting of this mutant compared to the fully myristoylated SHOC2<sup>S2G</sup> and the limited EGF-stimulated nuclear translocation of the non-myristoylated SHOC2<sup>S2G/ΔKEKE</sup> protein (Figure 3C and Supplementary Material, Fig. S3).

### SHOC2<sup>S2G</sup> dynamically associates with lipid rafts

RAS proteins, which are targeted to the plasma membrane by different C-terminal anchors, operate in functionally distinct microdomains (24,25). Among these, the lipid rafts are tightly packed cholesterol/sphingolipid-rich domains, which are more ordered than the surrounding lipid bilayer. These specialized subdomains serve as sorting platforms, reservoirs for inactive signalling proteins or hubs for signal transduction to mediate specific recruitment of proteins, facilitate compartmentalization of signalling in the membrane, or mediate RAS signalling tuning (26–28). Localization of RAS in lipid rafts is dynamic. Specifically, palmitoylated HRAS localizes in lipid rafts in its inactive state, and its translocation to cholesterol-independent domains is necessary for efficient activation of the MAPK cascade (27,29). In contrast, NRAS displays an opposite relocation following stimulation (30). This differential spatial localization is likely to account, in part, for the diverse signal outputs promoted by these proteins (31). Since plasma membrane targeting of SHOC2<sup>S2G</sup> represents a key event in the enhanced and prolonged activation of MAPK signalling, membrane microdomain partitioning of the myristoylated mutant was analysed in lysates of transiently transfected Neuro2A cells starved and stimulated with EGF or left untreated (Figure 4). Sucrose gradient ultracentrifugation was used to separate the detergent-insoluble lipid rafts, which float to low-density fractions of the gradient (32,33), and fractions were then analysed by western blotting to verify the presence of the protein by using flotillin as a lipid raft marker (34,35). In line with previous observations, in starved condition, HRAS was present in the insoluble fractions containing lipid rafts (fractions 4–6) as well as in soluble fractions (fractions 7–9), the latter including proteins located in other membrane domains

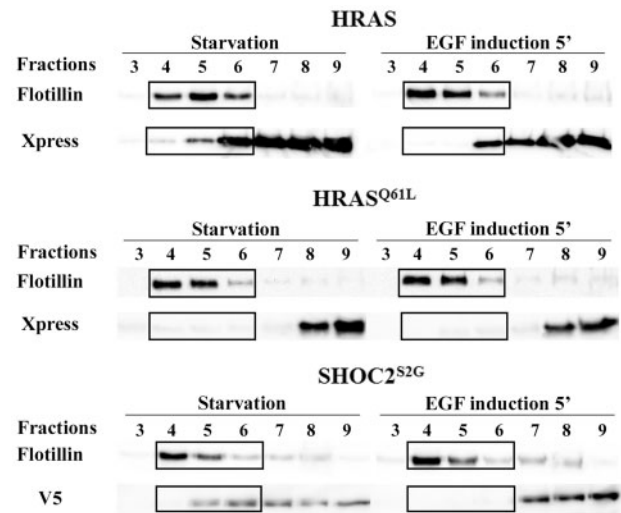


**Figure 4.** Membrane microdomain partitioning of the N-myristoylated SHOC2<sup>S2G</sup> mutant. SHOC2<sup>S2G</sup> (bottom panel) localizes in both insoluble fractions (fraction 4–6, containing lipid rafts) and soluble fractions (fractions 7–9, including other membrane domains and cytosol) basally; a redistribution of the scaffold protein from rafts to non-raft domains of the plasma membrane occurs following stimulation. This behavior is similar to what was observed for the HRAS GTPase (top panel). The constitutive localization of the hyperactive HRAS<sup>Q61L</sup> mutant in soluble fractions is shown for comparison (middle panel). The detergent-insoluble lipid rafts were separated by sucrose gradient ultracentrifugation, and fractions were analysed by western blotting using flotillin as lipid raft marker. Analyses were performed in transiently transfected Neuro2A cells starved, and then stimulated with EGF or left untreated.

or in the cytosol (Figure 4, top panel). EGF stimulation of cells resulted in a redistribution of the GTPase from rafts to non-raft domains of the plasma membrane. Consistent with the observed HRAS re-distribution following stimulation, a constitutively activated HRAS mutant, HRAS<sup>Q61L</sup>, was observed to localize exclusively in fractions not containing lipid rafts (Figure 4, middle panel). Similarly to what was documented for the wild-type HRAS protein, a dynamic association of SHOC2<sup>S2G</sup> with lipid rafts was observed, with a translocation of the mutant in cholesterol-independent membrane subdomains following stimulation (Figure 4, bottom panel). We tested two membrane-targeted mutants, SHOC2<sup>S2G/ΔKEKE</sup> and SHOC2<sup>S2G/ALRR11-14</sup>, and observed that they redistributed to raft and non-raft domains dynamically, similar to that of the myristoylated SHOC2<sup>S2G</sup> protein (data not shown). These results indicated that deletion of the KEKE motifs or LRRs located at the C-terminus do not impact substantially the interaction with proteins residing in these subdomains of the plasma membrane.

### SHOC2's LRR motifs constitute two structurally recognizable and tandemly arranged domains

Our findings indicated differential roles for the N-terminal and C-terminal LRRs in controlling SHOC2 subcellular localization and modulation of RAS-MAPK signalling, suggesting that these motifs may be organized into two structurally distinct domains. To explore this possibility, a three-dimensional model of the tandemly arranged LRR motifs was built using the SWISS-MODEL automated protein structure homology modelling server. The model showed a similar orientation and curvature of all LRRs 1 to 20, even though a different spacing between LRRs 13 and 14 was apparent (Figure 5A). Molecular dynamics simulations (300 ns) performed to verify the stability of the

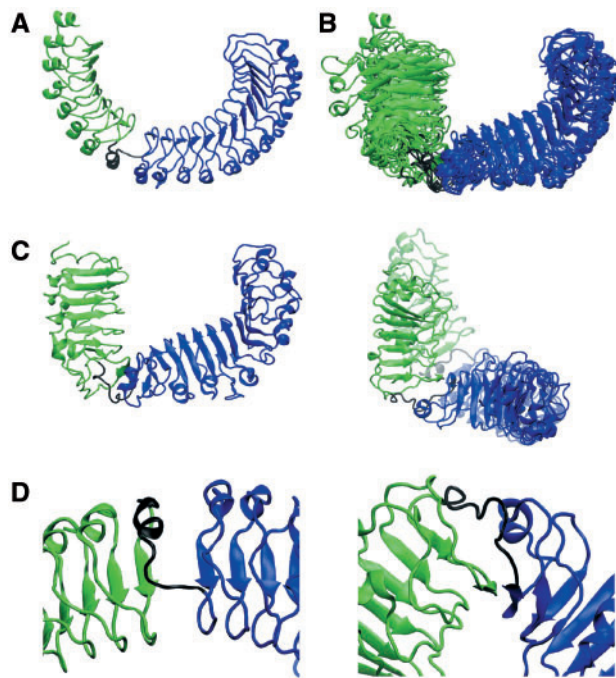


**Figure 5.** SHOC2's LRR motifs constitute two structurally recognizable and tandemly arranged domains. (A) Three-dimensional model of the tandemly arranged LRR motifs built using the SWISS-MODEL server. (B) Molecular dynamics simulations (300 ns) performed to verify the stability of the generated model documenting a very well-conserved  $\beta$  structure of individual LRRs in their conserved region. (C) The LRRs appear to be structured into two blocks (LRRs 1–13, and LRRs 14–20). (D) During the simulation, the variable region of LRR 13 rearranges structurally and appears to function as a flexible hinge between the two domains.

generated model documented well-conserved  $\beta$  structures of individual LRRs in their conserved region (Figure 5B; Supplementary Material, Fig. S5). Remarkably, during the simulation, rotation of LRRs 14 to 20, which were structured to form a single block with respect to LRRs 1 to 12 and the conserved region of LRR 13, constituting a distinct and stable domain, was observed (Figure 5C). In this simulation, the variable region of LRR 13 was observed to lose its starting secondary structure and to function as a flexible hinge between the two domains (Figure 5D). LRR 13 showed variability in the length of the  $\beta$  structure in the conserved LRR region, in line with their position at the boundary of the two domains (Supplementary Material, Fig. S5).

Overall, consistent with the experimental data, *in silico* structural and molecular dynamics data support the idea that LRRs 1–13 and LRRs 14–20 constitute two structurally independent domains that are connected by a flexible hinge constituted by the variable region of LRR 13. In this structural organization, we expect the presence of residues playing a major role in favouring the flexibility of the linker connecting the two LRR domains and plasticity of their relative orientation. Of note, LRR 13 lacks the leucine residue at the C-terminus of its variable region and the leucine residue at the N-terminus of the conserved region of LRR 14 is replaced by methionine, suggesting a possible structural relevance of the observed amino acid substitutions at these key positions.

## Discussion

In this study, we dissected the functional and structural organization of SHOC2 by identifying the domains required for

constitutive plasma membrane targeting of the RASopathy-causing SHOC2<sup>S2G</sup> mutant and those controlling the nuclear import and export of the wild-type protein. We also determined the impact of subcellular mis-localization of the scaffold on ERK signalling and more precisely characterized the SHOC2's module architecture of its tandemly arranged LRR motifs. Finally, we showed that SHOC2<sup>S2G</sup> dynamically associates with lipid rafts and translocates to cholesterol-independent domains following stimulation.

SHOC2 is a protein functioning as a positive modulator of the RAS-MAPK signalling cascade (1,2,36). While conflicting data support its ability to bind to multiple members of the RAS subfamily (1,4,6), it is largely accepted that SHOC2's positive modulatory role on ERK activation is exerted by accelerating stable interaction between RAS and RAF1 (5,6). Consistent with these findings, siRNA-mediated depletion of SHOC2 has been shown to dramatically decrease the extent of stimulus-induced ERK activation (37), and ubiquitination and degradation of SHOC2 has recently been documented to represent an event negatively controlling RAF1 catalytic activation (38). Intriguingly, besides the established role of the scaffold in RAS-MAPK signalling, a still uncharacterized function of SHOC2 in the nucleus has been postulated (7). We excluded the presence of a functionally active NLS in the protein, and confocal microscopy analysis and cell fractioning experiments with cells expressing an opportunely generated panel of SHOC2 mutants lacking the N-terminal KEKE motifs-rich region (residues 7–56) or a different subset of the tandemly arranged LRRs allowed us to identify the functional domain of the protein implicated in SHOC2's nucleocytoplasmic shuttling. Specifically, we showed that the first 10 LRRs are required for SHOC2 import into the nucleus, while the N-terminal KEKE motif-rich region of the protein is necessary to achieve efficient nuclear export of the protein. These data, which are in line with our previous observations (7), support a specific role of SHOC2 in the nucleus in response to EGF stimulation. Consistent with our finding, SHOC2 is predicted as a putative nuclear protein by PSORT II (<http://psort.hgc.jp/form2.html>), and is classified with similar confidence as having a nuclear localization or as a protein shuttling between the cytosol and nucleus by WoLF PSORT (nucl: 19, cyto\_nucl: 18.5, cyto: 12) (39).

SHOC2's positive function in RAS-MAPK signalling has been linked to its ability to bind to PP1C, favouring the translocation of this serine/threonine protein phosphatase to the membrane, where dephosphorylation of Ser<sup>259</sup> of RAF1 is required to stabilize RAF1 binding to RAS and proper activation of the kinase (6). Consistent with this view, a virtually invariant amino acid substitution, p.Ser2Gly, promoting SHOC2 myristoylation, and multiple missense mutations affecting Ser<sup>259</sup> (or adjacent residues) of RAF1 have been identified as the molecular causes of two clinically related RASopathies, and associated with variably upregulated MAPK signalling (7,40). In the former, myristoylation has been shown to result in constitutive mis-targeting of the scaffold to the plasma membrane; in the latter, loss of Ser<sup>259</sup> has been documented to destabilize the autoinhibited RAF1 conformation mediated by 14-3-3 protein binding to pSer<sup>259</sup>, promoting stable binding of the kinase to GTP-bound RAS (41). As in our previous observations, we failed to observe a substantial localization of wild-type SHOC2 at the plasma membrane, which is in apparent conflict with the direct role of this scaffold in mediating stable RAF1 interaction with RAS proteins. Notwithstanding this apparent incongruence, the present data confirm the activating role of the Ser2Gly substitution on SHOC2 as well as the dependence of its positive modulating role on

ERK activation and targeting of the protein to the plasma membrane. Our present and previous observations are consistent with a model in which SHOC2 translocation to the membrane in response to factor stimulation is transient and possibly required only as priming for RAF1 activation.

Previous work using red fluorescent protein-(RFP) tagged SHOC2 attempted to characterize the subcellular localization of SHOC2 and the role of the SHOC2<sup>S2G</sup> mutant on ERK signalling (37). This group documented a diffuse distribution of the protein in both cytoplasm and nucleus basally, and its translocation to a subpopulation of late endosomes following EGF stimulation, which is in contrast with the present and our previous observations. Galperin and colleagues also reported data not supporting the activating role of the RASopathy-causing mutant on ERK signalling. While the use of a relatively large sized tag (i.e. RFP), might account for the remarkable diverse picture compared with the present data, particularly taking into account the relatively low molecular weight of SHOC2 and the relatively weak interactions characterizing SHOC2 (our unpublished observations), the contrasting data produced using different experimental tools and approaches do required further investigation. In a subsequent work, the same group utilized an approach based on the generation of truncated RFP-tagged mutants to map the role of individual SHOC2's structural elements on the subcellular localization of the scaffold (42). In this case, the different generated constructs do not allow a direct comparison of the gathered data with the present findings. It should be considered, however, that the high molecular weight and possible steric hindrance of the tag used for these analyses are expected to dramatically impact on subcellular localization and protein-protein interactions of the generated truncated mutants.

While N-terminal myristoylation is a modification largely used to anchor proteins to intracellular membranes, its binding energy is relatively weak. Stable binding of N-myristoylated proteins to intracellular membranes generally requires additional non-covalent interaction(s) with phospholipids of the cytoplasmic leaflet of the bilayer or other membrane-bound proteins. Similarly, the non-specific hydrophobic interaction mediated by N-myristoylation does not explain the constitutive targeting of SHOC2<sup>S2G</sup> to the plasma membrane. SHOC2 does not possess positively charged regions potentially implicated in phospholipids binding nor cysteine residues that might provide additional acylation contributing to membrane binding stabilization. By evaluating the subcellular localization of a series of truncated SHOC2<sup>S2G</sup> mutants by confocal microscopy and cell fractioning experiments, we provided evidence showing that the N-terminal LRR motifs constituting the first LRR domain are also required for constitutive mis-targeting of myristoylated SHOC2<sup>S2G</sup> to the plasma membrane. This finding indicates that this domain has a crucial role in mediating SHOC2's protein-protein interactions mediating translocation of the protein to different intracellular compartments as well as its dynamic association with lipid rafts.

Consistent with the gathered experimental data, our *in silico* structural and molecular dynamics analyses support a previously unappreciated organization of SHOC2's LRRs to constitute two structurally independent domains coupled by a flexible hinge. This structural organization provides a structural framework for the appreciated distinct role of the N- and C-terminal LRRs in mediating protein-protein interactions controlling SHOC2 intracellular localization and modulation of ERK signalling. A systematic analysis of the role of the different residues in the flexibility of the two domains is expected to identify the structure-dynamics determinants governing the hinge role of LRR 13.

A major finding of this study is the observation that SHOC2 trapping at different subcellular sites differentially impacts ERK signalling strength and dynamics. These data also provide the first hint for a possible dual counteracting modulatory role of this protein on ERK signalling, with a negative control exerted in the nucleus. In this model, besides the established role of the scaffold for promoting the PP1C-mediated RAF1 dephosphorylation at Ser<sup>259</sup> and the priming event required for the activation of the kinase, SHOC2 could function also as a negative modulator of ERK signalling following its translocation in the nucleus. In this manner, constitutive mis-targeting of SHOC2<sup>S2G</sup> to the plasma membrane is expected to promote ERK signalling by both favouring prolonged RAF1 dephosphorylation at Ser<sup>259</sup> and defective down-modulation of signalling in the nucleus. Based on these considerations, we anticipate that a different class of mutations specifically affecting proper nuclear internalization of SHOC2 might have clinical relevance and underlie a mild phenotype within the RASopathy phenotypic spectrum.

## Materials and Methods

### Reagents

Dulbecco's modified Eagle's medium (DMEM), fetal bovine serum (FBS), phosphate-buffered saline (PBS), glutamine and antibiotics were obtained from Euroclone (Wetherby, UK). Fugene6 transfection reagent and Complete protease inhibitor cocktail tablets were purchased from Roche Diagnostics (Mannheim, Germany). MG132 was from Sigma-Aldrich (St. Luis, MO). [9,10-<sup>3</sup>H(N)] myristic acid was from PerkinElmer (Santa Clara, CA). Nuclear Extract kit was purchased from Active Motif (Carlsbad, CA). Dual-Luciferase Reporter Assay System was obtained from Promega (Madison, WI). Trans-Blot Turbo Transfer Packs were from Bio-Rad Laboratories (Hercules, CA). ECL Western Blotting Detection reagents were obtained from Pierce Biotechnology (Rockford, IL). QuikChange Site-Directed Mutagenesis kit was obtained from Stratagene (La Jolla, CA). pcDNA6/V5-HisA eukaryotic expression vector and epidermal growth factor (EGF) were from Invitrogen (Carlsbad, CA). The following antibodies were used: mouse monoclonal anti-V5 and anti-Xpress (Invitrogen); mouse monoclonal anti-β-Actin and horseradish peroxidase-conjugated anti-rabbit or anti-mouse (Sigma-Aldrich); mouse monoclonal anti-HA and rabbit polyclonal anti-YY1 (Santa Cruz Biotechnology, Santa Cruz, CA); rabbit polyclonal anti-Na/K-ATPase and mouse monoclonal anti-Phospho-p44/42 MAPK (Thr202/Tyr204) (Cell Signaling Technology, Danvers, MA); mouse monoclonal anti-Flotillin-1 (BD Transduction Laboratories, Franklin Lakes, NJ); anti-mouse conjugated to Alexa Fluor 594 (Molecular Probes, Eugene, OR). Alexa Fluor 488 phalloidin dye was from Molecular Probes. Vectashield antifade medium containing DAPI was purchased from Vector Laboratories (Burlingame, CA).

### Constructs

Plasmids encoding wild-type SHOC2 carrying three amino acid substitutions (p.P79A, p.R82G, p. K83G) in predicted NLS (SHOC2<sup>P79A/R82G/K83G</sup>) and SHOC2<sup>S2G</sup> mutated in the putative palmitoylation site (p.C144G) (SHOC2<sup>S2G/C144G</sup>) were generated by site-directed mutagenesis. The first was obtained using the pcDNA6/V5-SHOC2 construct as template and the following primer pair: P79A/R82G/K83G-Fw 5'-G CCA AAC CCA GCA GCT GGG ACT GGA GGA AAA TCC AGC AAT GC-3' and P79A/R82G/K83G-Rv 5'-GC ATT GCT GGA TTT TGC TCC AGT CCC AGC TGC TGG

GTT TGG C-3'. The second was obtained utilizing pcDNA6/V5-SHOC2<sup>S2G</sup> construct as template and the following primer pair: C144G-Fw 5'-C CCA GCA GAG GTG GGA GGT TTA GTA AAT CTC-3' and C144G-Rv 5'-GAG ATT TAC TAA ACC TCC CAC CTC TGG G-3'.

The SHOC2<sup>AKEKE</sup> and SHOC2<sup>S2G/AKEKE</sup> constructs were produced by PCR and cloning of the amplification products into the pcDNA6/V5-HisA expression vector using the following primer pairs: *NheI*\_KEKE-Fw 5'-GCT AGC ACC ATG AGT AGT AGT TTA GGA AAA GAA AAG GAC TCC AGT GCT GCC CAA C-3' and *XhoI*\_SHOC2-Rv 5'-CTC GAG GAC CAT GGC ACG ATA TGG ACC-3', and *NheI*\_KEKE-Fw 5'-GCT AGC ACC ATG GGT AGT AGT TTA GGA AAA GAA AAG GAC TCC AGT GCT GCC CAA C-3' and *XhoI*\_SHOC2-Rv, respectively.

Plasmids for expression of SHOC2 mutants with partial deletions of the LRR region (SHOC2<sup>ALRR2-5</sup>, SHOC2<sup>ALRR6-10</sup>, SHOC2<sup>ALRR11-14</sup> and SHOC2<sup>ALRR15-19</sup>) were generated by overlap extension PCR (43). Briefly, for each construct, two PCR products representing the flanking regions of the DNA sequence to be deleted were prepared using the following primer pairs: *NheI*\_SHOC2-Fw 5'-GCT AGC GAG TTC ATG TAG TTT TTG TCC AG-3', SHOC2<sup>ALRR2-5</sup>-Rv 5'-CT GAG TTT TGA CAA CTC TTT GAT TG-3' and SHOC2<sup>ALRR2-5</sup>-Fw 5'-CA ATC AAA GAG TTG TCA AAA CTC AG-3', *XhoI*\_SHOC2-Rv (the encompassing the deleted region); *NheI*\_SHOC2-Fw, SHOC2<sup>ALRR6-10</sup>-Rv 5'-CT ATT CAG TTT CAA GTT TTT GAT G-3' and SHOC2<sup>ALRR6-10</sup>-Fw 5'-C ATC AAA AAC TTG AAA CTG AAT AG-3', *XhoI*\_SHOC2-Rv (the encompassing the deleted region); *NheI*\_SHOC2-Fw, SHOC2<sup>ALRR11-14</sup>-Rv 5'-C CTC AAG AGA AAC CAC AAG ACT TG-3' and SHOC2<sup>ALRR11-14</sup>-Fw 5'-CA AGT CTT GTG GTT TCT CTT GAG G-3', *XhoI*\_SHOC2-Rv (the encompassing the deleted region); *NheI*\_SHOC2-Fw, SHOC2<sup>ALRR15-19</sup>-Rv 5'-GAT TGA AAG CTT GAG ACC AGA C-3' and SHOC2<sup>ALRR15-19</sup>-Fw 5'-G TCT GGT CTC AAG CTT TCA ATC-3', *XhoI*\_SHOC2-Rv (the encompassing the deleted region). In the next step, the two PCR products were used as a template for a ligation PCR containing the outermost primer pair (*NheI*\_SHOC2-Fw and *XhoI*\_SHOC2-Rv). Finally, each amplified fragment was cloned into the pcDNA6/V5-HisA.

Plasmids coding SHOC2<sup>S2G</sup> proteins with partial deletions of the LRR domain (SHOC2<sup>S2G/ALRR2-5</sup>, SHOC2<sup>S2G/ALRR6-10</sup>, SHOC2<sup>S2G/ALRR11-14</sup> and SHOC2<sup>S2G/ALRR15-19</sup>) were produced by site-directed mutagenesis using pcDNA6/V5-SHOC2<sup>ALRR2-5</sup>, pcDNA6/V5-SHOC2<sup>ALRR6-10</sup>, pcDNA6/V5-SHOC2<sup>ALRR11-14</sup> or pcDNA6/V5-SHOC2<sup>ALRR15-19</sup> vector as template and the following primer pair: SHOC2<sup>S2G</sup>-Fw 5'-C CAG GCT TGA GTC ACC ATG GGT AGT AGT TTA GGA AAA G-3' and SHOC2<sup>S2G</sup>-Rv 5'-C TTT TCC TAA ACT ACT ACC CAT GGT GAC TCA AGC CTG G-3'. The identities of all constructs were verified by bidirectional sequencing (ABI BigDye terminator Sequencing Kit v3.1 and ABI Prism 3500 Genetic Analyzer, Applied Biosystems).

### Cell culture, transfection and EGF stimulation

COS-1, HEK293, NIH 3T3 and Neuro2A cells (American Type Culture Collection, Manassas, VA, USA) were cultured in DMEM supplemented with 10% heat-inactivated FBS, 2 mM glutamine, 100 units/ml of penicillin and 100 µg/ml of streptomycin, and maintained at 37 °C in a humidified atmosphere containing 5% CO<sub>2</sub>. Subconfluent cells were transfected using the Fugene6 transfection reagent according to the manufacturer's instructions. In all experiments, serum-free DMEM and EGF (30 ng/ml) were utilized to starve and stimulate cells, respectively.

### Cell homogenate and protein assay

Neuro2A cells, transfected with the various constructs for 24 h, serum starved overnight and stimulated with EGF for the indicated intervals, were lysed in radioimmunoprecipitation assay (RIPA) buffer, pH 8.0, containing 20 mM NaF, 1 mM Na<sub>3</sub>VO<sub>4</sub> and protease inhibitors. Lysates were kept on ice (30 min) and then centrifuged at 16,000g (20 min, 4 °C). Supernatants were collected and their protein concentration was determined by bicinchoninic acid (BCA) assay (44), using bovine serum albumin (BSA) as a standard.

### Western blotting

Cell lysates were resolved by 7.5% sodium dodecyl sulphate (SDS)-polyacrylamide gel. After electrophoresis, proteins were transferred to nitrocellulose membrane using the Trans-Blot Turbo transfer system (Bio-Rad Laboratories). Blots were blocked with 5% non-fat milk powder in PBS containing 0.1% Tween-20 for 1 h and incubated with specific antibodies for 1 h. Primary and secondary antibodies were diluted in blocking solution. Immunoreactive proteins were detected by an enhanced chemiluminescence (ECL) detection kit, according to the manufacturer's instructions. Densitometric analysis of protein bands was performed using Alpha View SA image software (Protein Simple, Santa Clara, CA, USA).

### Cell fractionation

In nucleus-cytoplasm fractionation assays, cytoplasmic and nuclear fractions were obtained using the Nuclear Extract Kit. Briefly, transfected COS-1 cells were cultured in the presence of FBS or serum starved overnight and then stimulated with EGF or left untreated. Cells were washed with ice-cold PBS containing phosphatase inhibitors and removed from dish by gently scraping with cell lifter. The cell suspension was centrifuged at 150g (5 min, 4 °C) and the resulting pellet was resuspended in hypotonic buffer supplemented with 5% of detergent. After centrifugation (14,000g, 1 min, 4 °C), the cytoplasmic fraction was collected and the nuclear pellet was solubilized in complete lysis buffer [10% Dithiothreitol (DTT), 1% protease inhibitor cocktail, lysis buffer). Identical ratios, representing the same percentage of each subcellular fraction, were subjected to SDS-PAGE followed by western blotting, in order to represent the cellular ratio of the SHOC2 distribution in each compartment. To ensure no cross-contamination between the fractions, the same membrane was probed with antibodies to β-Actin (cytoplasmic marker) or YY1 (nuclear marker).

In nucleus-cytoplasm-membrane fractionation assays, transfected COS-1 cells were washed twice with PBS and harvested using buffer A (20 mM Tris-HCl, pH 7.4, 2 mM EDTA, protease inhibitor cocktail). After sample centrifugation (2,000g, 10 min, 4 °C), the supernatant consisting of cytoplasm and membranes was collected and again centrifuged (30,000g, 1 h, 4 °C). The nuclear pellet was resuspended in buffer A containing 1% Triton X-100 and 60 mM octyl-β-D-glucopyranoside (buffer B), passed 10 times through a syringe needle and then centrifuged (16,000g, 30 min, 4 °C). Finally, the cytoplasmic fraction was recovered and the pellet consisting of membranes was solubilized in buffer B. Identical ratios, representing the same percentage of each subcellular fraction, were subjected to SDS-PAGE followed by western blotting, in order to represent the cellular ratio of the SHOC2 distribution in the different cellular compartments. To ensure no cross-contamination between the

fractions, the same membrane was probed with antibodies to  $\beta$ -Actin (cytoplasmic marker), YY1 (nuclear marker) or Na/K-ATPase (plasma membrane marker).

### Dual-luciferase assay

ELK transcriptional activity was assessed using the Dual-luciferase reporter assay system. Briefly, NIH 3T3 cells were transfected with the appropriate SHOC2 construct, pFR-Luc reporter plasmid and pFA2-Elk1 fusion trans-activator vector. Renilla luciferase plasmid (pRLTk) was co-transfected as an internal transfection control. After 24 h, cells were serum starved overnight and stimulated with EGF for 6 h or left untreated. Lysates were centrifuged at 12,000g (1 min, 4°C) and supernatants were used for measurements of luciferase expression using a Microlite TLX1 luminometer (Dynatech Laboratories, Chantilly, VA).

### Isolation of lipid raft-enriched membrane fractions

Lipid raft-enriched membrane fractions were isolated as previously described (45). Briefly, Neuro2A cells were transfected with different constructs for 24 h, starved 4 h, stimulated with EGF or left untreated, rinsed twice with cold PBS and harvested in MES-buffered saline [(MBS) 25 mM 2-(N-morpholino) ethanesulfonic acid, pH 6.5, 150 mM NaCl] containing 1% Triton X-100, 1mM Na<sub>3</sub>VO<sub>4</sub> and protease inhibitors. Each cell lysate was Dounce homogenized, adjusted to 40% sucrose and placed at the bottom of an ultracentrifuge tube. A 5–30% linear sucrose gradient was then placed above the homogenate and the mixture was centrifuged at 45,000 rpm for 18 h at 4°C in a SW60Ti rotor (Beckman Instruments, Palo Alto, CA, USA). Twelve fractions were harvested from top of gradient and stored at –20°C until analysis.

### N-myristoylation analysis

COS-1 cells were transfected with SHOC2<sup>S2G</sup>, SHOC2<sup>S2G/AKEKE</sup> or SHOC2<sup>S2G/ALRR2-5</sup> construct for 24 h, washed twice with serum-free DMEM and incubated in DMEM with 2% FBS containing [<sup>3</sup>H]myristic acid (30  $\mu$ Ci/ml) for 5 h. Subsequently, the cells were lysed in ice-cold RIPA buffer supplemented with protease inhibitors, the lysates were centrifuged at 16,000g (20 min, 4°C) and the supernatants were used for immunoprecipitation with anti-V5 antibody. Samples were subjected to SDS-PAGE followed by western blotting or fluorography.

### Confocal laser scanning microscopy

COS-1 cells ( $30 \times 10^3$ ) were seeded on glass coverslips, transfected with the various constructs for 24 h, serum starved for 16 h and stimulated with EGF for 15 min. Cells were fixed with 3% paraformaldehyde for 30 min at 4°C and permeabilized with 0.5% Triton X-100 for 10 min at room temperature. Cells were then incubated with a specific mouse monoclonal primary antibody (anti-V5) for 1 h at room temperature, rinsed twice with PBS and incubated with the secondary anti-mouse antibody conjugated with Alexa Fluor 594 for 1 h at room temperature. Alexa Fluor 488 phalloidin dye was used to stain the cortical actin associated with the plasma membrane. Finally, glass coverslips were mounted on microscope slides using the Vectashield antifade medium containing DAPI and analysed by a Leica TCS SP2 AOBs apparatus, utilizing excitation spectral laser lines at

405, 488 and 594 nm, tuned with an acousto-optical tunable filter. Image acquisition and processing were conducted using the Leica Confocal Software 2.3 (Leica Lasertechnik, Heidelberg, Germany) and Adobe Photoshop 7.0 (Adobe Systems Incorporated, San Jose, CA, USA). Signals from different fluorescent probes were taken in sequential scanning mode.

### Model generation and simulation protocol

The 3D structure of the native SHOC2 protein was designed using the SWISS-MODEL automated protein structure homology modelling server (<http://swissmodel.expasy.org>) on template PDB Id: 4MN8 with high resolution 3.06 Å. In order to increase the protein model confidence, we carried out a molecular dynamics simulations with the Gromacs 4.5.6 package (46) and the gromos54a7.ff force field (47). The starting structures were embedded in a dodecahedron box, extending up to 12 Å from the solute, and immersed in SPC water molecules (48). Counter ions were added to neutralize the overall charge with the genion gromacs tool. After energy minimizations, the systems were slowly relaxed for 5 ns by applying positional restraints of 1000 kJ mol<sup>-1</sup> nm<sup>-2</sup> to the protein atoms. Then unrestrained MD simulations were carried out for a length of 300 ns with a time step of 2 fs. V-rescale temperature coupling was employed to keep the temperature constant at 300 K (49). The Particle-Mesh Ewald method was used for the treatment of the long-range electrostatic interactions (50). LRR motif annotation was performed according to (3) and (51).

### Supplementary Material

Supplementary Material is available at HMG online.

Conflict of Interest Statement. None declared.

### Funding

This work was supported by grants from AIRC (IG 17583), E-Rare (NSEuroNet), Telethon (GGP13107), and Ministero della Salute (RF-2011-02349938 and RC2016) to M.T.

### References

- Selfors, L.M., Schutzman, J.L., Borland, C.Z. and Stern, M.J. (1998) soc-2 encodes a leucine-rich repeat protein implicated in fibroblast growth factor receptor signaling. *Proc. Natl. Acad. Sci. USA*, **95**, 6903–6908.
- Sieburth, D.S., Sun, Q. and Han, M. (1998) SUR-8, a conserved Ras-binding protein with leucine-rich repeats, positively regulates Ras-mediated signaling in *C. elegans*. *Cell*, **94**, 119–130.
- Bella, J., Hindle, K.L., McEwan, P.A. and Lovell, S.C. (2008) The leucine-rich repeat structure. *Cell. Mol. Life Sci.*, **65**, 2307–2333.
- Li, W., Han, M. and Guan, K.L. (2000) The leucine-rich repeat protein SUR-8 enhances MAP kinase activation and forms a complex with Ras and Raf. *Genes Dev.*, **14**, 895–900.
- Matsunaga-Udagawa, R., Fujita, Y., Yoshiki, S., Terai, K., Kamioka, Y., Kiyokawa, E., Yugi, K., Aoki, K. and Matsuda, M. (2010) The scaffold protein Shoc2/SUR-8 accelerates the interaction of Ras and Raf. *J. Biol. Chem.*, **285**, 7818–7826.
- Rodriguez-Viciano, P., Oses-Prieto, J., Burlingame, A., Fried, M. and McCormick, F. (2006) A phosphatase holoenzyme comprised of Shoc2/Sur8 and the catalytic subunit of PP1

- functions as an M-Ras effector to modulate Raf activity. *Mol. Cell*, **22**, 217–230.
7. Cordeddu, V., Di Schiavi, E., Pennacchio, L.A., Ma'ayan, A., Sarkozy, A., Fodale, V., Cecchetti, S., Cardinale, A., Martin, J., Schackwitz, W., et al. (2009) Mutation of SHOC2 promotes aberrant protein N-myristoylation and causes Noonan-like syndrome with loose anagen hair. *Nat. Genet.*, **41**, 1022–1026.
  8. Tartaglia, M., Zampino, G. and Gelb, B.D. (2010) Noonan syndrome: clinical aspects and molecular pathogenesis. *Mol. Syndromol.*, **1**, 2–26.
  9. Roberts, A.E., Allanson, J.E., Tartaglia, M. and Gelb, B.D. (2013) Noonan syndrome. *Lancet*, **381**, 333–342.
  10. Mazzanti, L., Cacciari, E., Cicognani, A., Bergamaschi, R., Scarano, E. and Forabosco, A. (2003) Noonan-like syndrome with loose anagen hair: A new syndrome? *Am. J. Med. Genet. A*, **118A**, 279–286.
  11. Boutin, J.A. (1997) Myristoylation. *Cell. Signal*, **9**, 15–35.
  12. Farazi, T.A., Waksman, G. and Gordon, J.I. (2001) The biology and enzymology of protein N-Myristoylation. *J. Biol. Chem.*, **276**, 39501–39504.
  13. Resh, M.D. (1999) Fatty acylation of proteins: new insights into membrane targeting of myristoylated and palmitoylated proteins. *Biochim. Biophys. Acta*, **1451**, 1–16.
  14. Resh, M.D. (2006) Trafficking and signaling by fatty-acylated and prenylated proteins. *Nat. Chem. Biol.*, **2**, 584–590.
  15. Peitzsch, R.M. and McLaughlin, S. (1993) Binding of acylated peptides and fatty acids to phospholipid vesicles: pertinence to myristoylated proteins. *Biochemistry*, **32**, 10436–10443.
  16. Resh, M.D. (2001) Membrane targeting of lipid modified signal transduction proteins. *Subcell. Biochem.*, **37**, 217–232.
  17. Sigal, C.T., Zhou, W., Buser, C., McLaughlin, S. and Resh, M.D. (1994) Amino-terminal basic residues of Src mediate membrane binding through electrostatic interaction with acidic phospholipids. *Proc. Natl. Acad. Sci. USA*, **91**, 12253–12257.
  18. Zhou, W., Parent, L.J., Wills, J.W. and Resh, M.D. (1994) Identification of a membrane-binding domain within the amino-terminal region of human immunodeficiency virus type 1 Gag protein which interacts with acidic phospholipids. *J. Virol.*, **68**, 2556–2569.
  19. Alland, L., Peseckis, S.M., Atherton, R.E., Berthiaume, L. and Resh, M.D. (1994) Dual myristylation and palmitoylation of Src family member p59fyn affects subcellular localization. *J. Biol. Chem.*, **269**, 16701–16705.
  20. Wolven, A., Okamura, H., Rosenblatt, Y. and Resh, M.D. (1997) Palmitoylation of p59fyn is reversible and sufficient for plasma membrane association. *Mol. Biol. Cell*, **8**, 1159–1173.
  21. Macara, I.G. (2001) Transport into and out of the nucleus. *Microbiol. Mol. Biol. Rev.*, **65**, 570–594.
  22. Perutz, M. (1994) Polar zippers: their role in human disease. *Protein Sci.*, **3**, 1629–1637.
  23. Realini, C., Rogers, S.W. and Rechsteiner, M. (1994) KEKE motifs. Proposed roles in protein-protein association and presentation of peptides by MHC class I receptors. *FEBS Lett.*, **348**, 109–113.
  24. Niv, H., Gutman, O., Kloog, Y. and Henis, Y.I. (2002) Activated K-Ras and H-Ras display different interactions with saturable nonraft sites at the surface of live cells. *J. Cell. Biol.*, **157**, 865–872.
  25. Plowman, S.J., Muncke, C., Parton, R.G. and Hancock, J.F. (2005) H-ras, K-ras, and inner plasma membrane raft proteins operate in nanoclusters with differential dependence on the actin cytoskeleton. *Proc. Natl. Acad. Sci. U S A*, **102**, 15500–15505.
  26. Roy, S., Luetterforst, R., Harding, A., Apolloni, A., Etheridge, M., Stang, E., Rolls, B., Hancock, J.F. and Parton, R.G. (1999) Dominant-negative caveolin inhibits H-Ras function by disrupting cholesterol-rich plasma membrane domains. *Nat. Cell. Biol.*, **1**, 98–105.
  27. Prior, I.A., Harding, A., Yan, J., Sluimer, J., Parton, R.G. and Hancock, J.F. (2001) GTP-dependent segregation of H-ras from lipid rafts is required for biological activity. *Nat. Cell. Biol.*, **3**, 368–375.
  28. Nicolau, D.V., Jr., Burrage, K., Parton, R.G. and Hancock, J.F. (2006) Identifying optimal lipid raft characteristics required to promote nanoscale protein-protein interactions on the plasma membrane. *Mol. Cell. Biol.*, **26**, 313–323.
  29. Prior, I.A., Muncke, C., Parton, R.G. and Hancock, J.F. (2003) Direct visualization of Ras proteins in spatially distinct cell surface microdomains. *J. Cell. Biol.*, **160**, 165–170.
  30. Roy, S., Plowman, S., Rotblat, B., Prior, I.A., Muncke, C., Grainger, S., Parton, R.G., Henis, Y.I., Kloog, Y. and Hancock, J.F. (2005) Individual palmitoyl residues serve distinct roles in H-ras trafficking, microlocalization, and signaling. *Mol. Cell. Biol.*, **25**, 6722–6733.
  31. Omerovic, J. and Prior, I.A. (2009) Compartmentalized signaling: Ras proteins and signalling nanoclusters. *FEBS J.*, **276**, 1817–1825.
  32. Simons, K. and Toomre, D. (2000) Lipid rafts and signal transduction. *Nat. Rev. Mol. Cell. Biol.*, **1**, 31–39.
  33. Pike, L.J. (2003) Lipid rafts: bringing order to chaos. *J. Lipid Res.*, **44**, 655–667.
  34. Bickel, P.E., Scherer, P.E., Schnitzer, J.E., Oh, P., Lisanti, M.P. and Lodish, H.F. (1997) Flotillin and epidermal surface antigen define a new family of caveolae-associated integral membrane proteins. *J. Biol. Chem.*, **272**, 13793–13802.
  35. Volonte, D., Galbiati, F., Li, S., Nishiyama, K., Okamoto, T. and Lisanti, M.P. (1999) Flotillins/cavatellins are differentially expressed in cells and tissues and form a heterooligomeric complex with caveolins in vivo. Characterization and epitope-mapping of a novel flotillin-1 monoclonal antibody probe. *J. Biol. Chem.*, **274**, 12702–12709.
  36. Leon, G., Sanchez-Ruiloba, L., Perez-Rodriguez, A., Gragera, T., Martinez, N., Hernandez, S., Anta, B., Calero, O., Garcia-Dominguez, C.A., Dura, L.M., et al. (2010) Shoc2/Sur8 protein regulates neurite outgrowth. *PLoS One*, **9**, e114837.
  37. Galperin, E., Abdelmoti, L. and Sorkin, A. (2012) Shoc2 is targeted to late endosomes and required for Erk1/2 activation in EGF-stimulated cells. *PLoS One*, **7**, e36469.
  38. Jang, E.R., Shi, P., Bryant, J., Chen, J., Dukhande, V., Gentry, M.S., Jang, H., Jeoung, M. and Galperin, E. (2014) HUWE1 is a molecular link controlling RAF-1 activity supported by the Shoc2 scaffold. *Mol. Cell. Biol.*, **34**, 3579–3593.
  39. Horton, P., Park, K.J., Obayashi, T., Fujita, N., Harada, H., Adams-Collier, C.J. and Nakai, K. (2007) WoLF PSORT: protein localization predictor. *Nucleic Acids Res.*, **35**, W585–W587.
  40. Pandit, B., Sarkozy, A., Pennacchio, L.A., Carta, C., Oishi, K., Martinelli, S., Pogna, E.A., Schackwitz, W., Ustaszewska, A., Landstrom, A., et al. (2007) Gain-of-function RAF1 mutations cause Noonan and LEOPARD syndromes with hypertrophic cardiomyopathy. *Nat. Genet.*, **39**, 1007–1012.
  41. Muslin, A.J. (2005) Role of raf proteins in cardiac hypertrophy and cardiomyocyte survival. *Trends Cardiovasc. Med.*, **15**, 225–229.
  42. Jeoung, M., Abdelmoti, L., Jang, E.R., Vander Kooi, C.W. and Galperin, E. (2013) Functional Integration of the Conserved Domains of Shoc2 Scaffold. *PLoS One*, **8**, e66067.

43. Lee, J., Lee, H.J., Shin, M.K. and Ryu, W.S. (2004) Versatile PCR-mediated insertion or deletion mutagenesis. *BioTechniques*, **36**, 398–400.
44. Smith, P.K., Krohn, R.I., Hermanson, G.T., Mallia, A.K., Gartner, F.H., Provenzano, M.D., Fujimoto, E.K., Goeke, N.M., Olson, B.J. and Klenk, D.C. (1985) Measurement of protein using bicinchoninic acid. *Anal. Biochem.*, **150**, 76–85.
45. Sargiacomo, M., Sudol, M., Tang, Z. and Lisanti, M.P. (1993) Signal transducing molecules and glycosyl-phosphatidylinositol-linked proteins form a caveolin-rich insoluble complex in MDCK cells. *J. Cell Biol.*, **122**, 789–807.
46. Pronk, S., Páll, S., Schulz, R., Larsson, P., Bjelkmar, P., Apostolov, R., Shirts, M.R., Smith, J.C., Kasson, P.M., van der Spoel, D., et al. (2013) GROMACS 4.5: a high-throughput and highly parallel open source molecular simulation toolkit. *Bioinformatics*, **29**, 845–854.
47. Schmid, N., Eichenberger, A., Choutko, A., Riniker, S., Winger, M., Mark, A. and van Gunsteren, W. (2011) Definition and testing of the GROMOS force-field versions 54A7 and 54B7. *Eur. Biophys. J.*, **40**, 843–856.
48. Berendsen, H.J.C., Postma, J.P.M., van Gunsteren, W.F. and Hermans, J. (1981) In *Intermolecular Forces*. Pullman, Dordrecht, p. 331.
49. Bussi, G., Donadio, D. and Parrinello, M. (2007) Canonical sampling through velocity rescaling. *J. Chem. Phys.*, **126**, 014101.
50. Darden, T., York, D. and Pedersen, L. (1993) Particle mesh Ewald: An  $N \log(N)$  method for Ewald sums in large systems. *J. Chem. Phys.*, **98**, 10089.
51. Kobe, B. and Kajava, A.V. (2001) The leucine-rich repeat as a protein recognition motif. *Curr. Opin. Struct. Biol.*, **11**, 725–732.